ACS APPLIED MATERIALS & INTERFACES

RESEARCH ARTICLE

www.acsami.org

Creation of Biofunctionalized Micropatterns on Poly(methyl methacrylate) by Single-Step Phase Separation Method

Quoc-Phong Ho, Shu-Ling Wang, and Meng-Jiy Wang*

Department of Chemical Engineering, National Taiwan University of Science and Technology, 43 Keelung Road, Section 4, Taipei 106, Taiwan

Supporting Information

ABSTRACT: In this study, the polymer thin films containing micropatterns and biological functionalities were created by one-step procedure. The adjustable compositions among poly(methyl methacrylate) (PMMA), solvents, nonsolvent, and additional macromolecules formed the polymer thin films with different diameters ranging from 5 to 37 μm. The influences of topographical and chemical cues were investigated by directly cultivating L-929 fibroblasts on the prepared samples. The results revealed the predominant effect of surface topography that the cell density of L-929 fibroblasts increased proportionally with the average diameter of microconcaves. The cell number raised significantly on the PMMA thin films containing type I collagen and dopamine, with or without microstructures. On the other hand, the addition of bovine serum albumin in PMMA limited the growth of cells. The surface chemical composition and cell responses were evaluated by electron spectroscopy for chemical analysis (ESCA), viability assay, and immunostaining, respectively. This work proposed a simple and effective approach to incorporate the biological functions and surface topography simultaneously onto surface of materials that provided further applications for biomedical materials.

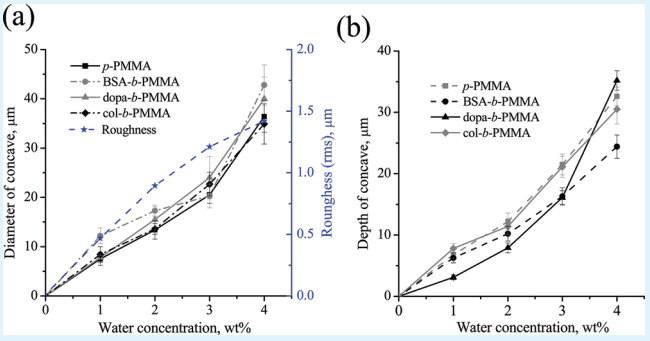

KEYWORDS: bovine serum albumin, collagen, dopamine, micropattern, microstructure, single-step phase separation

INTRODUCTION

The development of functional biomaterials requires searching for applicable substances which allow activating specific characteristics of cells and tissues. The most essential prerequisite for biomaterials is to support cell viability which is advantageous for the subsequent cell proliferation and migration. The viability of adherent cells relates closely to its morphology which is mediated by transmembrane adhesion receptors and corresponding extracellular matrix (ECM) proteins.[1−7] However, because of the lack of receptor on the synthetic materials, the presence of protein is usually necessary for cell adhesion.[8] Fibroncetin, vitronectin, and laminin are recognized as adhesive proteins which promote cell adhesion,[9,10] whereas serum albumin,[9,11,12] and immunoglobin (IgG) were recognized to prevent cell adhesion on the surfaces. The strategies used to modulate biological responses on biomaterials also included the modifications of hydrophilicity or elasticity of materials,[13,14] the changes of type and ratio of copolymers, and the geometrical arrangements for network polymers.[15] Surface modification methods generally aimed to introduce specific surface functionalities for biomaterials and the main strategies included wet chemical treatments and dry processes. Various chemical methods such as chemical etching, polymer adsorption, and self-assembly monolayers allowed to roughen the surfaces or to provide specific surface functionalities.[16,17] Furthermore, corona discharge and thermal and plasma treatment methods involved no solvents were also employed to impart chemical moiety and to alter surface topography. The surface modification by integrating ECM proteins to mediate cell adhesion and behavior was demonstrated by the adsorption of different layers of ECM components, e.g., collagen and fibronectin, on substrates.[13,18]

In addition, there are growing number of reports focused on how the cells detect and response to the nano- and microtopography of substrate materials and the succeeding influences on the morphology and spreading upon cell arrangements, proliferation, apotosis and macrophage activation.[19−22] For example, it was shown that a specifically designed microenvironment supported the cellular regeneration and directed the formation and vascularization of tissue.[23] The micropatterned poly(lactic-co-glycolic acid (PLGA) films coated with collagen or laminin peptide promoted axon growth and provided a guidance effect on both early stage neurite outgrowth and elongation.[24]

The creation of regular patterns on polymer surfaces by using photo-lithography and soft-lithography methods usually involved clean room processes and lengthy experimental procedures.[25−30] The breath-figure template is a more cost and time effective method to create regular patterned films with relatively ease but

Received: September 2, 2011
Accepted: October 24, 2011
Published: October 24, 2011

was showed limitations by its sensitivity to humidity and can be prepared only on hydrophilic materials.[31−38] Wang et al. have firstly introduced the single-step phase separation method which is facile and less humidity sensitive for the preparation of poly(methyl methacrylate) and poly(L-lactide) polymer thin films with concave size ranged from 4 to 8 μm.[39,40] Moreover, the addition of surfactant and the control of water concentration proved to assist the fabrication of very regular patterns with different concave sizes on polymer thin films.[41]

In this study, collagen and dopamine, which are an extracellular matrix protein and a mussel-inspired adhesive molecule, were added into polymer solutions for the formation of micropatterned polymer thin films. The spatial distribution and aggregation of collagens were reported to attribute to the cellular signaling and development through integrins recognitions.[42,43] On the other hand, the self-polymerization of dopamine via oxidation or coordination bonds from catechol groups revealed its applicability to form adhesive layer on various solid surfaces.[44,45] The coating of polydopamine on different substrates demonstrated excellent results on promoting cell adhesion even on the well-known anti-adhesive polymer, poly(tetrafluoroethylene).[46]

A raised issue for the developed strategies is that sometimes the surface modification methods were limited by the specificity to a certain type of substrate materials and lacked the possibility to modulate surface chemistry and the microenvironment simultaneously. In this study, a single-step method to fabricate thin polymer films containing biofunctionality and microstructures simultaneously was reported. Micro-patterned concaves with collagen, dopamine, or bovine serum albumin (BSA) integrated polymer thin films were prepared on poly(methyl methacrylate). The objectives are to find out the effects resulted from the incorporation of macromolecules and from the changes in surface topography. The promotion of cell responses was demonstrated by higher cell density and well-spread cell morphology on surfaces composed concurrently of chemical and topographical niches via the integration of collagen or dopamine. On the contrary, the incorporation of BSA into polymer solution revealed the effect of down-regulating cell proliferation. The single-step micropatterning and biofunctionalization process presented here provides an effective method for creating highly defined microstructures for modulating the cell responses which is suitable for the developments of biomedical materials.

EXPERIMENTAL SECTION

Materials. Poly(methyl methacrylate) (PMMA, m.w.: 97,000), dopamine, tetrahydrofuran (THF) were purchased from Acros (USA). Type I collagen, kindly provided by Professor Wei-Bor Tsai from National Taiwan University, was extracted from bovine skin as previously described.[47] The chemicals used for lactate dehydrogease (LDH) method consisted of lactic acid, nicotinamide adenine dinucleotide (NAD^+), diaphorase, bovine serum albumin, sucrose, indonitrotetrazolium (INT), phosphate buffered saline (PBS), and Triton X-100 were purchased from Sigma-Aldrich, MO, USA.

Preparation of Patterned Thin Films with Blended or Coated Proteins. The patterned surfaces were prepared by single-step phase separation method.[41,48,49] Briefly, PMMA was dissolved in THF mixed with water in different concentrations. The micro-patterned thin film was produced by adding 6 ml of polymer solution into Petri dishes (10 cm in diameter) at 20 °C with 85 % relative humidity for 12 h. The protein blended polymer thin films were prepared by adding protein into polymer solution to form a mixture of 0.1 mg/mL concentration of protein. For the thin polymer films coated with proteins, the prepared thin films containing patterns were immobilized in 0.1 mg/mL protein in (PBS pH 7.4) at 37°C for 12 h and followed by extensive washing with PBS and DI water and dried in laminar flow. All the polymer thin films were sterilized by UV exposure for 30 min for both sides of sample.

Surface Characterizations. Scanning electron microscope (SEM) was applied to observe the morphology of patterned surfaces and L-929 cells (JEOL JSM-6300) at 20 kV. The size of patterns was analyzed by ImageJ software. The wettability of the surfaces was evaluated by measuring the static water contact angle (Sindatek, model 100F) with deionized water; at least five points were measured for each sample. The chemical composition of samples was determined by Electron Spectroscopy for Chemical Analysis on a Thermo VG Scientific Theta Probe Instrument using monochromatic source of Al−Kα (1,486.6 eV) as excitation sources, with pass energy of 50 eV. The characterizations were taken under takeoff angle of 53°, with under X-ray spot size of 400 μm.

Cell Culture. The cell culture of L-929 fibroblast cells was performed in a humidified incubator under 37 °C and 5% CO_2 control. All culture media were purchased from Sigma: Dulbecco's modified eagle medium (DMEM-high glucose) (56439C); trypsin, lyophilized powder (T4799); EDTA (E6758); fetal bovine serum (F2442); sodium bicarbonate (S5761); sodium pyruvate (P5280); and L-glutamine (G8540). The cultivation periods were 30 min, 1h, 2 h, 4 h, and 24 h, and 48 h with initial cell density of 20 000 cells/ml.

Cell Viability by Lactate Dehydrogenase (LDH) Assay. The cell density was determined by performing lactate dehydrogenase assay.[50−52] The attached cells were lysed with 100 μl of 1 % Triton X-100 in PBS. The reaction solution contained 0.3% NAD^+, 0.27% diaphorase, 0.03% bovine serum albumin, 1.2% sucrose and 0.02% iodonitrotetrazolium, and 3.6 % sodium lactate (all chemicals were purchased from Sigma). The optical density values were read at 490 nm by using enzyme-linked immunosorbent assay (ELISA, iMark Absorbance Reader, BioRad). A standard curve was obtained by plotting measured optical density of a series of cell solutions with known cell densities.

Immunofluorescent Staining. The L-929 fibroblasts were fixed on the patterned surfaces by immersion in a solution of 4 % paraformaldehyde in phosphate buffered saline (PBS, pH 7.4), and followed by permeabilized with 0.1% Triton X-100 at room temperature. Non-specific binding of proteins and antibodies was prevented by incubation with 0.5 % bovine serum albumin (BSA) solution in PBS overnight at 4°C. The actin filaments and nuclei of cells were stained with 165 nM of Rhodamine-conjugated phalloidin (R415, Molecular Probes, USA) and DAPI (1:1000 dilutions, S7113, Chemicon International, Inc., USA) for 20 min at room temperature. Confocal laser scanning microscopy (CLSM) was utilized to visualize the stained cells (Leica-SP2, Germany)

Statistical Analysis. The variations of the amount of adherent and proliferate cells were statistically analyzed by performing one-way analysis of variance (ANOVA), executed by Minitab statistical software®. Fisher's pairwise comparison test was applied to compare the cell density on different samples for p <0.05.

RESULTS AND DISCUSSION

This study proposed a one-step method to simultaneously incorporate macromolecules into the polymer thin films and create surface micro patterns. The addition of collagen, dopamine, and bovine serum albumin into PMMA polymer solution formed collagen-blended-PMMA (col-*b*-PMMA), dopamine-blended-PMMA (dopa-*b*-PMMA), and BSA-blended-PMMA (BSA-*b*-PMMA), respectively. Previous study indicated that the micro-concaved PMMA was obtained by dissolving PMMA in THF while the flat PMMA can be prepared by dissolving PMMA in toluene (Figure 1a).[41] By adding the macromolecules into PMMA solution and adjusting the concentration of non-solvent,

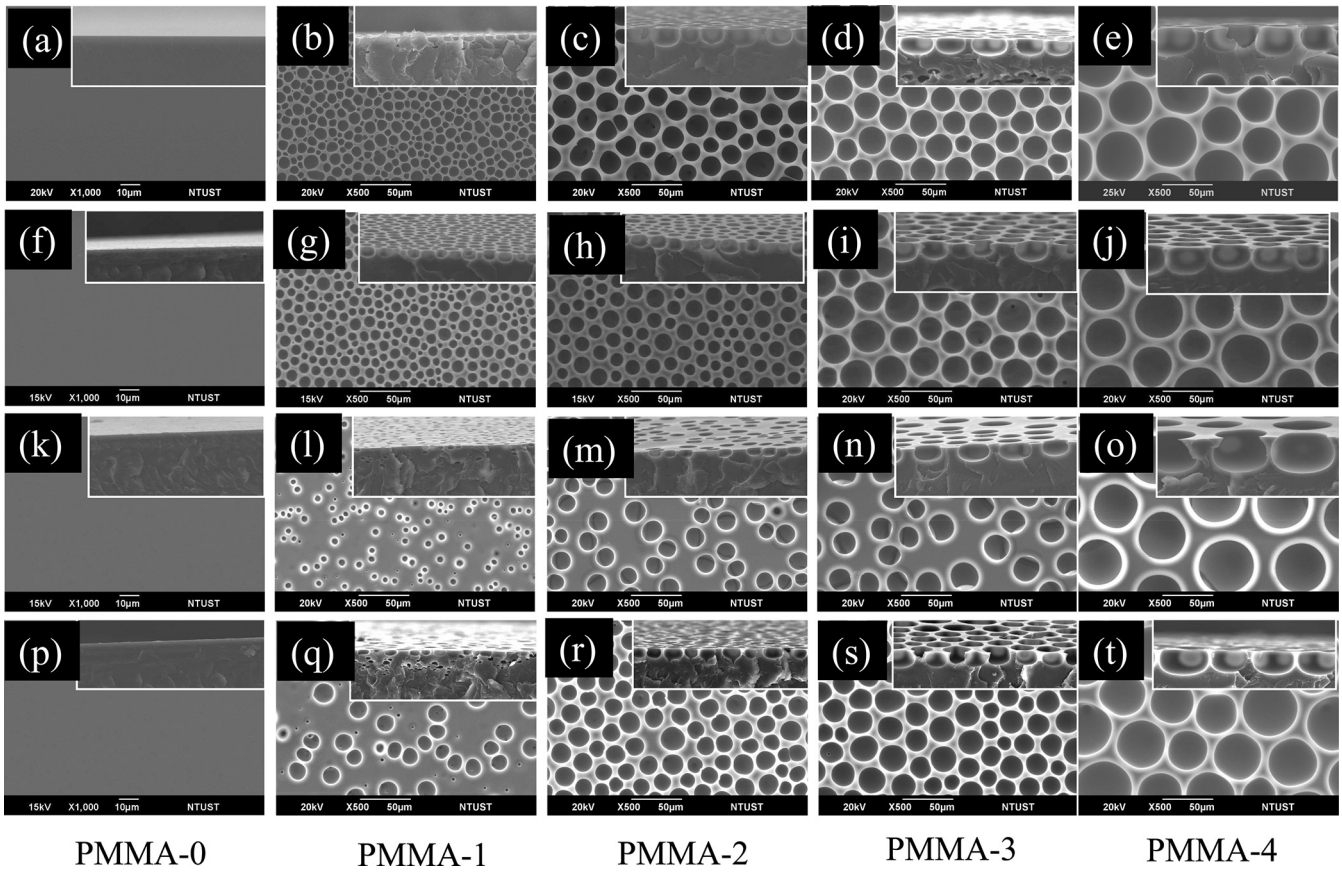

Figure 1. SEM images of concave patterned films: (a−e) *p*-PMMA (10 wt % in THF); (f−-j) col-*b*-PMMA (the PMMA solution contained 0.1 mg collagen/g solution); (k−o) dopa-*b*-PMMA (the PMMA solution contained 0.5 mg dopamine/g solution); (p−t) BSA-*b*-PMMA (the PMMA solution contained 0.1 mg BSA/g solution). (The films were prepared at 20°C. Inserts are the corresponding cross-sectional images. Scale bar = 10 μm for a, f, k, p and 50 μm for all the other figures.)

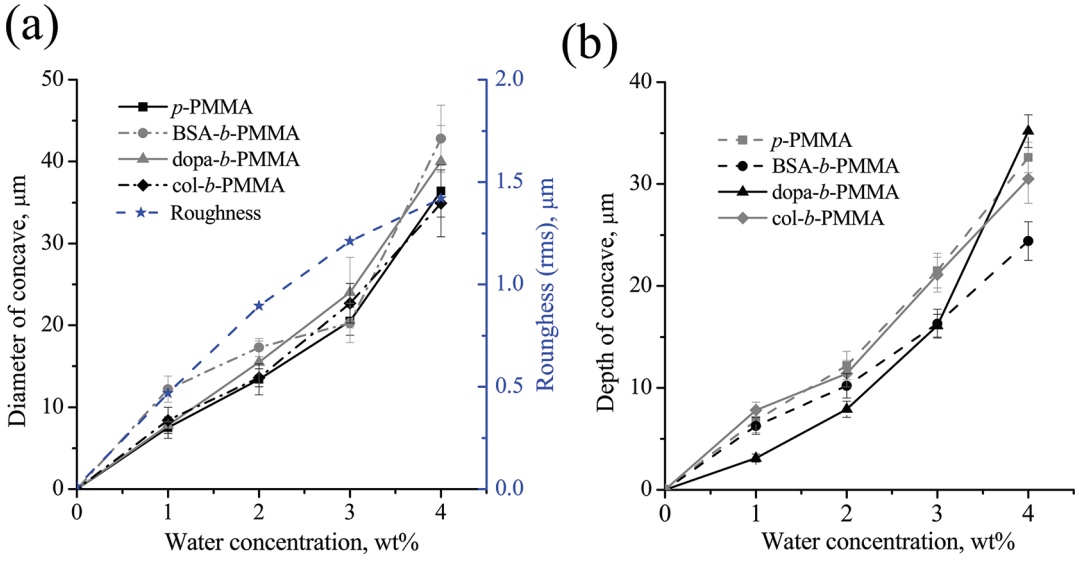

Figure 2. Correlations for patterned concaves: (a) the average diameter and surface roughness as function of water content and (b) the average depth of concave as function of water concentration.

the average diameter increased nearly linearly from 7.5 μm to 36.4 μm for PMMA polymer solution dissolved in THF and contained 1- 4 % of water (Figure 1, b-e), which were ascribed as PMMA-1, PMMA-2, PMMA-3, and PMMA-4, respectively. The mixing of macromolecules with polymer solutions showed limited effect on the size of concaves on that the

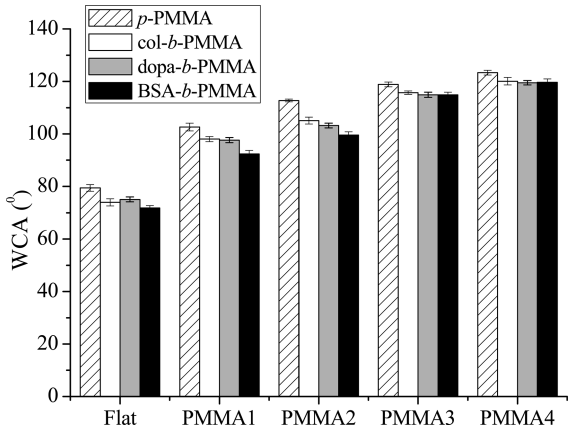

Figure 3. Water contact angle of samples containing micropatterns of different average diameter and biofunctionalities.

average diameter and the depth of the concaves are similar to that of pristine-PMMA (*p*-PMMA) (Figure 1g–j, l–o, q–t, and Figure 2). The results indicated that the size of concave was affected primarily by the composition among the solvent (THF), non-solvent (water), and solutes (macromolecules and PMMA) but not by the variation of the compositions of the solutes. The creation of identical size of patterns on polymer thin films with different type of macromolecules allows comparing the mammalian cell responses on materials with different functionalities under the same basis of surface microstructure. To discuss the effects of macromolecule blending, we assessed the surface characterizations and the L-929 fibroblast cell responses on the patterned thin films.

Surface Characterizations. The flat pristine PMMA showed a water contact angle (WCA) of 79.4°. The surface concaves on PMMA resulted in the increase of water contact angles to 102.6, 112.8, 118.9, and 123.4° for *p*-PMMA-1 to *p*-PMMA-4, respectively (Figure 3). The blending of collagen altered the flat PMMA to hydrophilic and the WCA decreased slightly to 73.9°. Moreover, the incorporation of collagen resulted in the decrease of WCA to 98.1, 105.1, 115.7, and 120.1° for col-*b*-PMMA-1 to col-*b*-PMMA-4, correspondingly. Similarly, the mixing of dopamine or BSA with PMMA solution caused about 5-10° decrease of WCA in comparison with the *p*-PMMA of different concave sizes. Figure 3 illustrated clearly that the PMMA became more hydrophilic due to the addition of collagen, dopamine, and BSA.

The pristine PMMA was composed of about 75% carbon and 25% oxygen regardless the existence of concaves, characterized by ESCA (Table 1). The blending of collagen, dopamine and BSA incorporated 1.5-1.8% of nitrogen, indicating the integration of macromolecules into the PMMA thin films. Moreover, the chemical composition revealed that the identical nitrogen contents and N/C ratios (~2%) by using the three molecules were obtained regardless the size of surface patterns, confirmed the equivalent observations from surface wettability characterized by WCA measurements.

Responses of Mammalian Cells on Micro Patterned Surfaces. The cell responses on the micropatterned PMMA with different concave diameter and integrated with various types of macromolecules was evaluated by directly cultivating mammalian cells on the samples and characterized by lactate dehydrogenase assay and confocal microscopy. The cell density was evaluated at different cell culture durations (0.5, 1, 2, and 24 h)

Table 1. Chemical Composition Analyzed by ESCA for Micropatterned PMMA with Different Diameter of Concaves and Biofunctionalities[a]

		samples	C 1s (%)	O 1s (%)	N 1s (%)	O/C (%)	N/C (%)
(a)	*p*-	PMMA0	75.1	24.9	0.0	33	0.0
		PMMA1	75.0	25.0	0.0	33	0.0
		PMMA2	73.3	26.6	0.0	36	0.0
		PMMA4	74.4	25.6	0.0	34	0.0
(b)	col-*b*	PMMA0	74.4	23.9	1.7	32	2.0
		PMMA1	74.5	23.8	1.7	32	2.0
		PMMA2	74.3	24.0	1.7	32	2.0
		PMMA4	74.4	24.0	1.7	32	2.0
(c)	dopa-*b*	PMMA0	76.7	21.7	1.6	28	2.0
		PMMA1	77.2	21.0	1.8	27	2.0
		PMMA2	76.6	21.9	1.5	29	2.0
		PMMA4	76.6	21.8	1.6	28	2.0
(d)	BSA-*b*	PMMA0	74.6	23.6	1.8	32	2.0
		PMMA1	74.5	23.8	1.7	32	2.0
		PMMA2	74.3	24.2	1.5	33	2.0
		PMMA4	72.1	26.5	1.5	37	2.0
(e)	col-*c*	PMMA0	72.2	23.0	4.8	31.9	6.6
		PMMA1	73.2	20.4	6.5	27.9	8.8
		PMMA2	72.1	21.5	6.4	29.9	8.9
		PMMA4	76.1	17.7	6.2	23.3	8.2
(f)	dopa-*b*-2	PMMA0	73.70	23.52	2.8	32	3.8
		PMMA1	73.43	23.58	3.0	32	4.1
		PMMA2	71.75	25.31	2.9	35	4.1
		PMMA4	70.13	26.94	2.9	38	4.2

[a] (a) *p*, pristine PMMA; (b) col-*b*, collagen blended; (c) dopa-*b*, dopamine blended; (d) BSA-*b*, BSA blended; (e) col-*c*, collagen coated; (f) dopa-*b*-2, dopamine blended with 4 folds of dopamine concentration in comparing with dopa-*b*.

and was normalized to the cell density on tissue-culture polystyrene (TCPS), served as the control group, with corresponding cell culturing time.

Effects of Topography on Cell Responses: LDH and Confocal Microscopy. The topographical effects on cell density were clearly observed in Figure 4. For short term cultivation time, the cell density increased significantly on the concave patterned films when compared to that on the flat ones. For example, after 2 h cell culture, the cell density increased to nearly 2- and 5-fold on PMMA-1 and PMMA-4 when compared to that on PMMA-0 (flat surface) for *p*-PMMA. Moreover, by 24 h cultivation time, the cell density increased correspondingly with the diameter of concaves. In comparison with PMMA-0, the cell density amplified from 1.2 to 1.8 folds for PMMA-1 to PMMA-4, respectively. The confocal microscopy images showed that the fibroblasts attached on *p*-PMMA-0 revealed circular shape and with limited number after 24 h cultivation (Figure 5a). The cell density increased approximately as function of the size of the concave on *p*-PMMA-1–*p*-PMMA-4 (Figure 5b-e), suggesting that the cell proliferation was promoted by the larger concave where the average diameter ranged from 7-37 μm in this study. For col-*b*-PMMA and dopa-*b*-PMMA, it is observed that a higher cell density was found on the surfaces contained larger diameter of concave, especially on col-*b*-PMMA-4 and dopa-*b*-PMMA-4

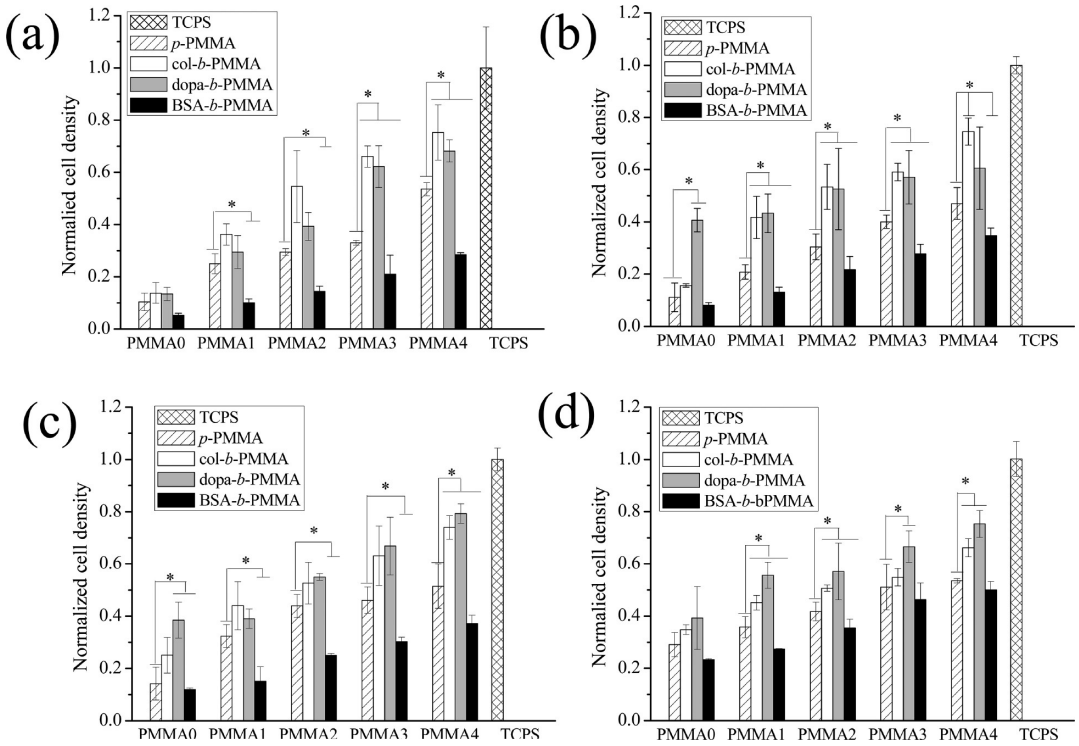

Figure 4. LDH results for the cell density on pristine (*p*-PMMA), collagen blended (col-*b*-PMMA), dopamine blended (dopa-*b*-PMMA), and BSA blended (BSA-*b*-PMMA) PMMA at different cultivation time: (a) 30 min, (b) 1 h, (c) 2 h, and (d) and 24 h. The cell density on col-*b*-PMMA, dopa-*b*-PMMA, and BSA-*b*-PMMA were compared with that on *p*-PMMA, indicated by (*) in which the significant values were showed with $p < 0.05$.

(Figure 5f–j and k–o). Although only limited number of cells was found on BSA blended PMMA thin films when compared with *p*-PMMA and collagen or dopamine blended PMMAs, the cell density increased as function of the diameter of concaves for BSA-*b*-PMMA (Figure 5, p-t). The lower cell density on the BSA blended PMMA was due to the possible surface passivation characteristic of BSA which prevented protein adsorption.[53]The observations led to an important remark that, within the average diameter of concaves discussed in this study, the topographical change itself governed the cell responses in a linear manner on the PMMA surfaces regardless the surface functionalities.

Effects of Biofunctionality on Cell Responses: LDH and Confocal Microscopy. For 0.5 h cell culturing period, the cell number increased slightly on the col-*b*-PMMA and dopa-*b*-PMMA thin films in comparison with *p*-PMMA (Figure 4a). The cell proliferation increased more significantly on PMMA-3 and PMMA-4 for collagen and dopamine blended PMMA. The incorporation of BSA revealed only inhibition effect on cell density for all samples, with or without surface concaves, to about 65-80 % of that on *p*-PMMA and only 33-80 % of that on col-*b*-PMMA and dopa-*b*-PMMA, respectively (Figure 4). The effects of ECM and adhesive molecules on the cell density were clearly revealed by confocal microscopy images that more cells were observed on the col-*b*-PMMA and dopa-*b*-PMMA when compared to that on *p*-PMMA and BSA-*b*-PMMA for either flat or surface patterned samples (Figure 5). The results confirmed the cell viability data analyzed by LDH assay. It is worthy to note that, although similar nitrogen content and N/C ratio was integrated by blending with collagen and BSA, the cell responded contradictorily, which might be due to the particular surface passivation characteristic of BSA, preventing further protein adsorption and following cell adhesion.[53] The results implied that the synergistic integration of structural niches and chemical functionalities into biomaterials, which mimic the in vivo microenvironment, provides a promising approach for the promotion or inhibition of the growth of mammalian cells.

The incorporation of surface functionalities were commonly achieved by immobilization, surface grafting, or surface modifications in which the immobilization is the simplest and effective method.[54−57] However, the preparation of surfaces with topographical clues and functionalities were usually performed in multiple experimental steps. In the study, a single process was employed to prepare the microstructured PMMA integrated with functionality. For the purpose of comparisons, the micropatterned PMMA coated with collagen (named as col-*c*-PMMA) that was prepared by taking more experimental procedures was also prepared. The collagen coating assisted the increase of cell density to about 2-fold within the first 4 h (Figure 6a). For the prolonged cell cultivation time, the cell density revealed more than 1.4 folds on the col-*c*-PMMA in comparison with the pristine and col-*b*-PMMA, especially on the PMMA with microstructures (see Figure S1b in Supplementary Information). The efficacy of the col-*c* was most probably due to the higher content of nitrogen via the immobilization method which was revealed from the ESCA results that more than 3 folds of nitrogen was found on the collagen coated samples when compared to the collagen blended ones, with and without surface microstructure (Table 1, samples b & e). The result revealed that the effect of coating was more important than that of blending for promoting cell growth. In addition, the more extended cell morphology with higher cell density was observed on the col-*c*-PMMA when compared to that on col-*b*-PMMA (Figure 7).

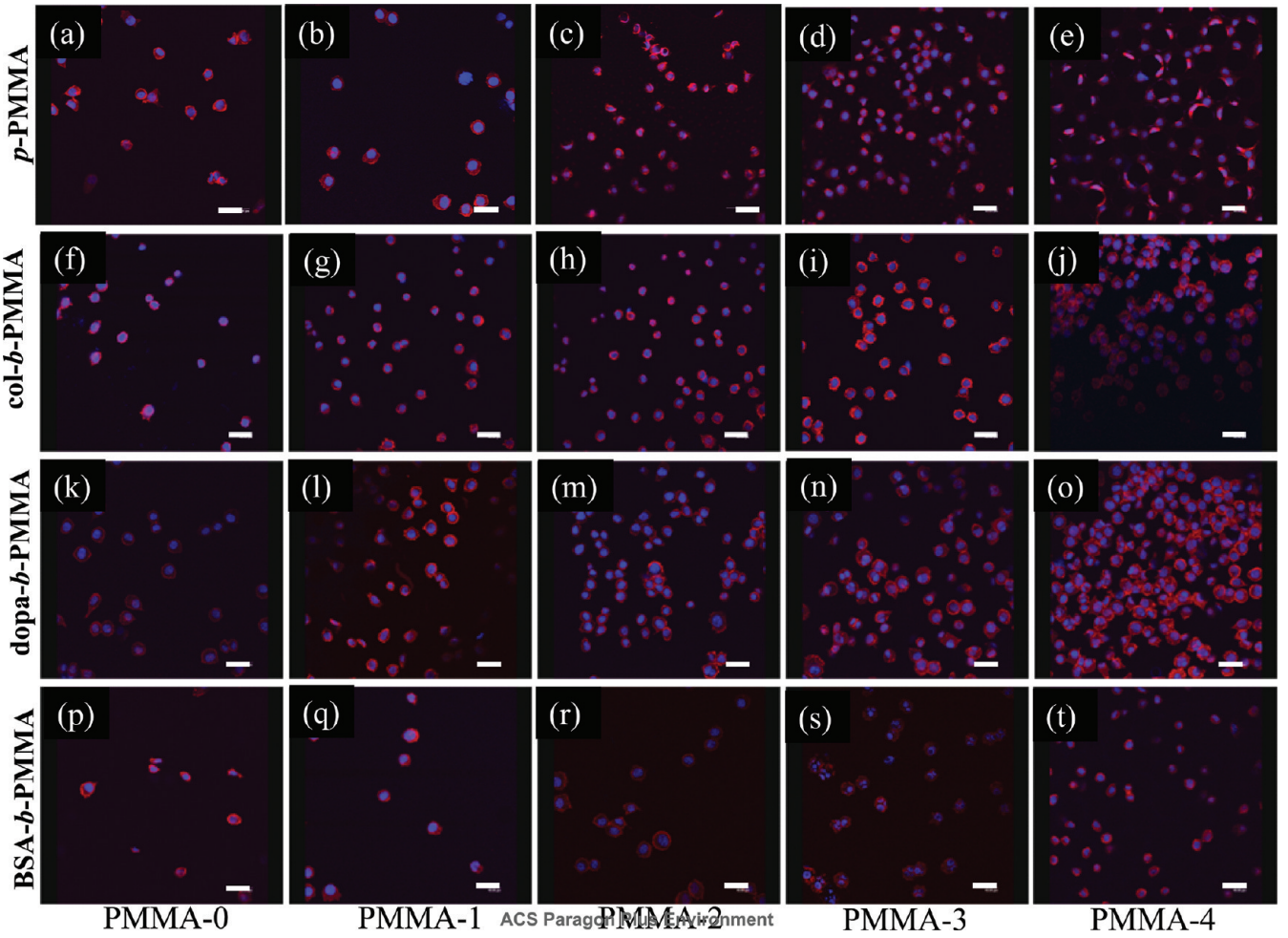

Figure 5. Confocal laser scanning microscopy images of L-929 fibroblasts on pristine PMMA, collagen-blended, dopamine-blended, and BSA-blended PMMA, cultured at 24 h: (a−e) *p*-PMMA, (f−j) col-*b*-PMMA, (k−o) dopa-*b*-PMMA, and (p−t) BSA-*b*-PMMA. The concave size of PMMA thin films: (a, f, k, p) PMMA-0, (b, g, l, q) PMMA-1, (c, h, m, r) PMMA-2, (d, i, n, s) PMMA-3, and (e, j, o, t) PMMA-4 (scale bar = 40 μm).

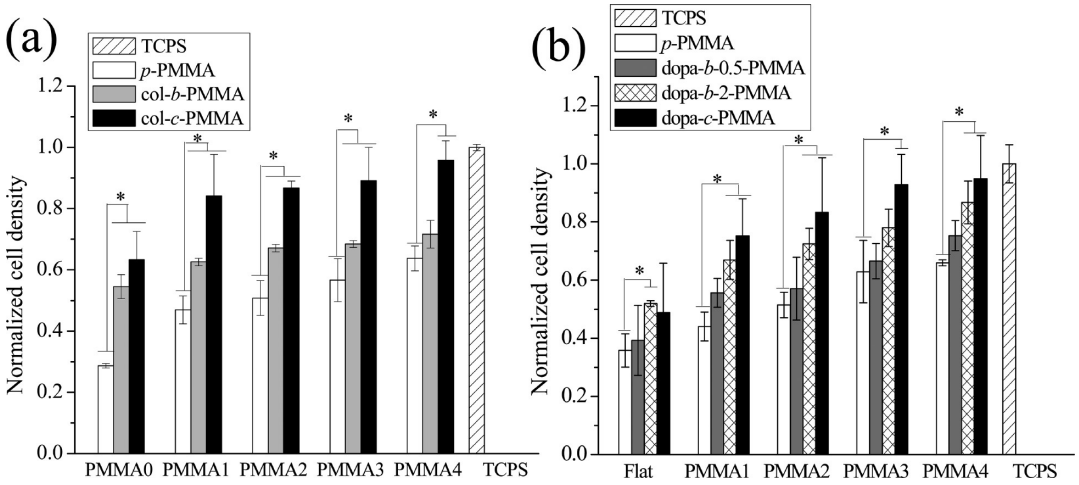

Figure 6. (a) LDH results for cell adhesion on coated (col-*c*-PMMA) and blended (col-*b*-PMMA) films for 24 h and (b) the cell density on samples with different amount of dopamine: dopa-*b*-0.5-PMMA , dopa-*b*-2-PMMA , and dopa-*c*-PMMA. The cell density on all samples was compared and normalized to that on *p*-PMMA, indicated by (*), in which significant values were shown with $p < 0.05$.

To verify the effects of nitrogen content on the cell responses, 4 folds of dopamine concentration was added into PMMA solution to form the dopa-*b*-2-PMMA with various size of concaves. The samples with higher dopamine concentration were prepared

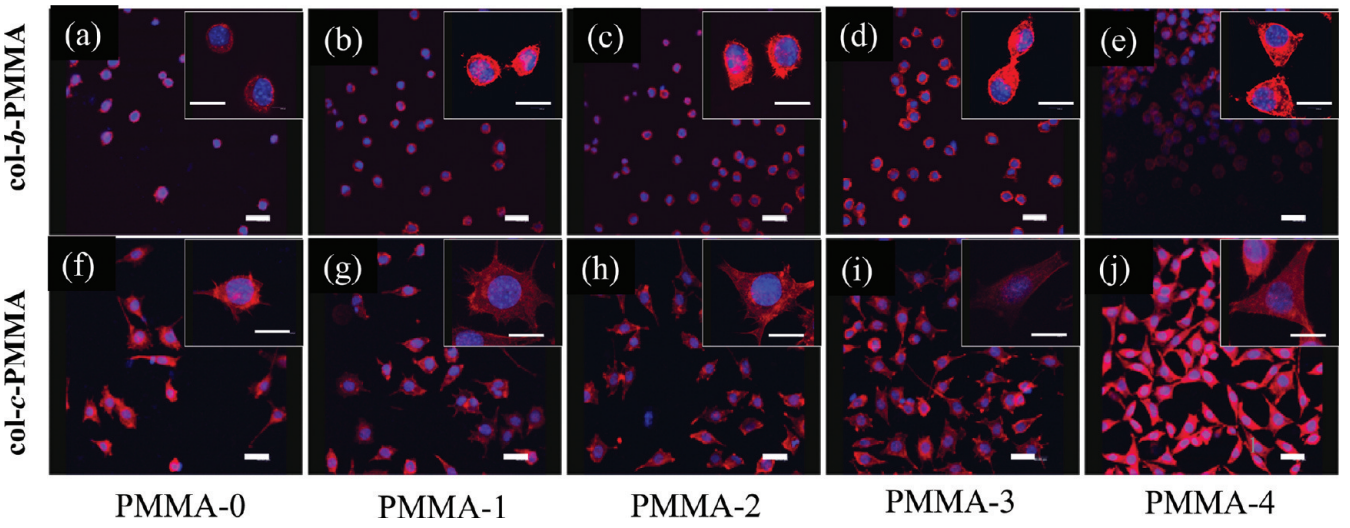

Figure 7. Confocal laser scanning microscopy images of L-929 fibroblasts on (a−e) col-*b*-PMMA and (f−j) col-*c*-PMMA, cultured for 24 h. The concave size of the PMMA thin films: (a, f) PMMA-0, (b, g) PMMA-1, (c, h) PMMA-2, (d, i) PMMA-3, and (e, j) PMMA-4 (scale bar = 40μm). The insets are the images with higher magnitudes for individual cells.

because dopamine is less expensive and is easier to be dissolved in PMMA/THF solution when compared to collagen. The blending of dopamine with 2 mg/mL assisted the increase of nitrogen content from 1.5 to 2.9 %, and the N/C ratios from 2.0 to 4.1% (Table 1, samples c & f). The increase of the dopamine concentration from 0.5 to 2 mg/mL was not reflected by ESCA analyses which only showed two folds increase of surface N/C ratio, indicating that the blending procedure resulted in the bulk distribution of the macromolecules. Moreover, the cell proliferation results revealed that, indeed, the higher nitrogen content of dopa-*b*-2-PMMA promoted effectively the increase of adherent cells in comparison with the dopa-*b*-PMMA (with lower blended dopamine concentration) (Figure 6b).The obtained results suggested that the surface topography and surface chemistry concurrently resulted in the intracellular organization which later dictated cell responses.

In summary, the experimental design used in this study by creating identical micropatterns on PMMA with different biofunctionalities, we found that (i) the micro topographical motif alone promoted the cell growth effectively that the cell density increased as function of the concave diameter within the range of 7−37 micrometer; (ii) the cell density was mostly affected by the surface micro structures during the first 4 h after cell seeding, usually recognized as the initial cell adhesion duration; (iii) the modulation of cell responses was achievable by choosing appropriate macromolecules to be incorporated into the polymer solution that the fixation of collagen and dopamine demonstrated the efficiency for supporting the growth of mammalian cells, especially for the first 4 h of cell culturing period, and (iv) the addition of bovine serum albumin revealed inhibition effect on cell growth at all time period in comparison with that on *p*-PMMA.

CONCLUSION

We demonstrated a facile and effective method to prepare biofunctionalized and micro patterned PMMA thin films in single step. The addition of macromolecules neither affected the formation of concave patterns nor altered the average size or depth of the patterned concaves. The creation of similar microstructure polymer thin films with different biofunctionalities provided a particular opportunity for the investigations focused on the surface chemistry of the patterned materials, which usually required sample preparations in multiple steps. The incorporation of extracellular matrix protein, type I collagen, and adhesion molecule dopamine promoted the cell growth whereas the addition of bovine serum albumin exhibited repelling effect on both cell adhesion and prolieferation. The comparisons of surface coating technology confirmed that the surface nitrogen content indeed played an important role for dictating the cell responses. Moreover, we have demonstrated that the adjustments of the concentrations of the added macromolecules into the polymer solutions further supported the control of the surface functionality of the micropatterned polymer thin films. The present study provides an unprecedented route to produce surface microstructures and biofunctionalities with one experimental step, which can be applied in fields of biomaterials and tissue engineering.

ASSOCIATED CONTENT

Supporting Information. Three-dimensional diagrams were drawn for the comparisons of cell responses on the PMMA surfaces with different topography and surface biofunctionalities. This material is available free of charge via the Internet at http://pubs.acs.org.

AUTHOR INFORMATION

Corresponding Author

*Tel: +886-2-2730-1146. Fax: +886-2-2737-6644. E-mail: mjwang@mail.ntust.edu.tw.

ACKNOWLEDGMENT

The authors express great appreciation to the National Science Council and National Taiwan University of Science and Technology for their financial support (NSC 99-2621-M-011-003).

REFERENCES

(1) Hynes, R. O. *Cell* **1987**, *48* (4), 549–554.
(2) Hynes, R.O. *Cell* **1992**, *69* (1), 11–25.

(3) Pavalko, F. M.; Otey, C.A. *Proc. Soc. Exp. Biol. Med.* **1994**, *205*, 282–293.
(4) Sastry, S. K.; Burridge, K. *Exp. Cell Res.* **2000**, *261* (1), 25–36.
(5) Geiger, B.; Bershadsky, A.; Pankov, R.; Yamada, K. M. *Nat. Rev. Mol. Cell Biol.* **2001**, *2* (11), 793–805.
(6) Hynes, R. O. *Cell* **2002**, *110* (6), 673–687.
(7) Wozniak, M. A.; Modzelewska, K.; Kwong, L.; Keely, P. J. *BBA—Mol. Cell Res.* **2004**, *1692* (2-3), 103–119.
(8) Chen, H.; Yuan, L.; Song, W.; Wu, Z.; Li, D. *Prog. Polym. Sci.* **2008**, *33* (11), 1059–1087.
(9) Tamada, Y.; Ikada, Y. *J. Colloid Interf. Sci.* **1993**, *155* (2), 334–339.
(10) Schmidt, D. R.; Waldeck, H.; Kao, W. J. In *Biological Interactions on Materials Surfaces*; Puleo, D. A., Bizios, R., Eds.; Springer: New York, 2009; p 1—18.
(11) Arima, Y.; Iwata, H. *Biomaterials* **2007**, *28* (20), 3074–3082.
(12) Deligianni, D. D.; Katsala, N.; Ladas, S.; Sotiropoulou, D.; Amedee, J.; Missirlis, Y. F. *Biomaterials* **2001**, *22* (11), 1241–1251.
(13) Krasteva, N.; Harms, U.; Albrecht, W.; Seifert, B.; Hopp, M.; Altankov, G.; Thomas, Groth. *Biomaterials* **2002**, *23* (12), 2467–2478.
(14) Boese, G.; Trimpert, C.; Albrecht, W.; Malsch, G.; Groth, T.; Lendlein, A. *Tissue Eng.* **2007**, *13* (12), 2995–3002.
(15) Scharnagl, N.; Lee, S.; Hiebl, B.; Sisson, A.; Lendlein, A. *J. Mater. Chem.* **2010**, *20* (40), 8789–8802.
(16) Love, J. C.; Wolfe, D. B.; Haasch, R.; Chabinyc, M. L.; Paul, K. E.; Whitesides, G. M.; Nuzzo, R. G. *J. Am. Chem. Soc.* **2003**, *125* (9), 2597–2609.
(17) Gao, Z. *Appl. Surf. Sci.* **2011**, *257* (14), 6068–6072.
(18) Berrier, A. L.; Yamada, K. M. *J. Cell Physiol.* **2007**, *213* (3), 565–573.
(19) Clark, P.; Connolly, P.; Curtis, A. S.; Dow, J. A.; Wilkinson, C. D. *Development* **1987**, *99* (3), 439–448.
(20) Britland, S.; Morgan, H.; Wojiak-Stodart, B.; Riehle, M.; Curtis, A.; Wilkinson, C. *Exp. Cell Res.* **1996**, *228* (2), 313–325.
(21) McCaig, C.; Rajnicek, A.; Britland, S. *J. Cell Sci.* **1997**, *110*, 2905–2913.
(22) Schwartz, Z.; Lohmann, C. H.; Vocke, A. K.; Sylvia, V. L.; Cochran, D. L.; Dean, D. D.; Boyan, B. D. *J. Biomed Mater. Res.* **2001**, *56* (3), 417–426.
(23) Peppas, N; Langer, R. *Science* **1994**, *263* (5154), 1715–1720.
(24) Engler, A. J.; Sen, S.; Sweeney, H. L.; Discher, D. E. *Cell* **2006**, *126* (4), 677–689.
(25) Shishido, A.; Diviliansky, B. I.; Khoo, I. C.; Mayer, T. S. *Appl. Phys. Lett.* **2001**, *79*, 3332–3334.
(26) Cao, T.; Wei, F.; Jiao, X.; Chen, J.; Liao, W.; Zhao, X.; Cao, W. *Langmuir* **2003**, *19* (20), 8127–8129.
(27) Altomare, L.; Gadegaard, N.; Visai, L.; Tanzi, M. C.; Farè, S. *Acta Biomaterialia* **2010**, *6* (6), 1948–1957.
(28) Hannachi, I. E.; Itoga, K.; Kumashiro, Y.; Kobayashi, J.; Yamato, M.; Okano, T. *Biomaterials* **2009**, *30* (29), 5427–5432.
(29) Rolland, J. P.; Hagberg, E. C.; Denison, G. M.; Carter, K. R.; Simone, J. M. D. *Angew. Chem., Int. Ed.* **2004**, *43*, 5796–5799.
(30) Connal, L. A.; Qiao, G.G. *Adv. Mater.* **2006**, *18*, 3024–3028.
(31) François, B.; Pitois, O.; François, J. *Adv. Mater.* **1995**, *7* (12), 1041–1044.
(32) Limaye, A. V.; Narhe, R. D.; Dhote, A. M.; Ogale, S. B. *Phys. Rev. Lett.* **1996**, *76* (20), 3762.
(33) Pitois, O.; François, B. *Eur. Phys. J. B - Condensed Matter and Complex Systems* **1999**, *8* (2), 225–231.
(34) de Boer, B.; Stalmach, U.; Nijland, H.; Hadziioannou, G. *Adv. Mater.* **2000**, *12* (21), 1581–1583.
(35) Peng, J.; Han, Y.; Yang, Y.; Li, B. *Polymer* **2004**, *45*, 447–452.
(36) Tian, Y.; Ding, H.; Jiao, Q.; Shi, Y. *Macromol. Chem. Phys.* **2006**, *207*, 545–553.
(37) Tung, P. H.; Kuo, S. W.; Jeong, K. U.; Cheng, S. Z. D.; Huang, C. F.; Chang, F. C. *Macromol. Rapid. Comm.* **2007**, *28* (3), 271–275.
(38) Zhao, B.; Zhang, J.; Wu, H.; Wang, X.; Li, C. *Thin Solid Films* **2007**, *515*, 3629–3634.
(39) Gao, J.; Kim, Y. M.; Coe, H.; Zern, B.; Sheppard, B.; Wang, Y. D. *Natl. Acad. Sci. U.S.A.* **2006**, *103* (45), 16681–16686.
(40) Pelling, A. E.; Dawson, D. W.; Carreon, D. M.; Christiansen, J. J.; Shen, R. R.; Teitell, M. A.; Gimzewski, J. K. *J. Nanomed. Nanotechnol.* **2007**, *3* (1), 43–52.
(41) Phong, H. Q.; Wang, S. L.; Wang, M. J. *Mater. Sci. Eng., B* **2010**, *169* (1-3), 94–100.
(42) Hui, T. Y.; Cheung, K. M.C.; Cheung, W. L.; Chan, D.; Chan, B. P. *Biomaterials* **2008**, *29* (22), 3201–3212.
(43) Lanfer, B.; Seib, F. P.; Freudenberg, U.; Stamov, D.; Bley, T.; Bornhäuser, M.; Werner, C. *Biomaterials* **2009**, *30* (30), 5950–5958.
(44) Zürcher, S.; Wäckerlin, D.; Bethuel, Y.; Malisova, B.; Textor, M.; Tosatti, S.; Gademann, K. *J. Am. Chem. Soc.* **2006**, *28* (4), 1064–1065.
(45) Wach, J. Y.; Malisova, B.; Bonazzi, S.; Tosatti, S.; Textor, M.; Zürcher, S.; Gademann, K. *Chem.—Eur J.* **2008**, *14* (34), 10579–10584.
(46) Ku, S. H.; Ryu, J.; Hong, S.K.; Lee, H.; Park, C. B. *Biomaterials* **2010**, *31* (9), 2535–2541.
(47) Tsai, S.; Hsu, F. Y.; Chen, P. L. *Acta Biomater.* **2008**, *4* (5), 1332–1341.
(48) Tian, Y.; Ding, H.; Shi, Y.; Jiao, Q.; Wang, X. *J. Appl. Polym. Sci.* **2006**, *100*, 1013–1018.
(49) Wang, Y.; Liu, Z.; Huang, Y.; Han, B.; Yang, G. *Langmuir* **2006**, *22*, 1928–1931.
(50) Tsai, W. B.; Grunkemeier, J. M.; Horbett, T. A. *J. Biomed. Mater. Res.* **1999**, *44* (2), 130–139.
(51) Tsai, W. B.; Lin, J. H. *Acta Biomater.* **2009**, *5* (5), 1442–1454.
(52) Tamada, Y; Kulik, EA; Ikada, Y. *Biomaterials* **1995**, *16* (3), 259–261.
(53) Sweryda-Krawiec, B.; Devaraj, H.; Jacob, G.; Hickman, J. J. *Langmuir* **2004**, *20* (6), 2054–2056.
(54) Amiji, M.; Park, K. *J. Biomater. Sci., Polym Ed.* **1993**, *4* (3), 217–234.
(55) Ikada, Y. *Biomaterials* **1994**, *15* (10), 725–736.
(56) Ito, Y. *Biomaterials* **1999**, *20* (23-24), 2333–2342.
(57) Cheng, Z.; Teoh, S. H. *Biomaterials* **2004**, *25* (11), 1991–2001.